Bacterial specific adhesion of Staphylococcus epidermidis onto human fibronectin under uniform flow by Grace Tein-ya Wang

A thesis submitted in partial fulfillment of the requirements for the degree of Doctor of Philosophy in Civil Engineering
Montana State University

Abstract:
Bacterial infection has drawn serious attention in modern medicine, either in respect to biomaterial infection or invasion of tissue surfaces in human bodies. Bacterial adhesion is an essential step in biofilm formation and subsequent infection. Among those factors involved in the complex adhesion process, specific adhesion is a major determinant of cell-cell and cell-substratum adhesions. Currently, the receptor:ligand theory is widely adopted as the governing mechanism of specific cell adhesion.

Staphylococcus epidermidis, a prevailing nosocomial pathogen of biomedical implants and devices, uses the specific adhesion binding with human fibronectin (FN), a glycoprotein found in extracellular matrix and plasma. A FN specific receptor on S. epidermidis and the protein FN pair as the receptor:ligand in specific adhesion. This dissertation reports an experimental study of the specific adhesion of S. epidermidis cells to fibronectin-coated substrata under uniform shear flow. The effects of ligand density on specific adhesion as well as the binding affinities between bacterial cells and different portions of the ligands were studied. The amount of FN molecule bound on the substratum was verified by radiolabeling. Results revealed that exposed NH2 functional groups of FN exhibited better binding affinity with S. epidermidis cells than to the FN molecule with -COOH functional groups free. Increases in FN density on the substratum with the NH2 groups exposed to bacterial cells led to increased rates and extent of bacterial adhesion.

A dynamic model, proposed in a previous work, was used to describe bacterial cell adhesion that is mediated by specific receptordigand binding. Computer simulations of specific adhesion were carried out by introducing the actual laboratory conditions and experimental parameters into the model to interpret the results. The computer simulations agreed well with the experiments with lower inlet cell concentration, while larger deviations existed in the range of higher inlet cell concentration.

BACTERIAL SPECIFIC ADHESION OF *Staphylococcus epidermidis* ONTO HUMAN FIBRONECTIN UNDER UNIFORM FLOW

by

Grace Tein-ya Wang

A thesis submitted in partial fulfillment
of the requirements for the degree

of

Doctor of Philosophy

in

Civil Engineering

MONTANA STATE UNIVERSITY-BOZEMAN
Bozeman, Montana

January 1999

APPROVAL

of a thesis submitted by

Grace Tein-ya Wang

This thesis has been read by each member of the thesis committee and has been found to be satisfactory regarding content, English usage, format, citations, bibliographic style, and consistency, and is ready for submission to the College of Graduate Studies.

James D. Bryers, Chair — James D Bryers — 10 Jan 99
Date

Approved for the Department of Civil Engineering

Don Rabern, Dept. Head — Don Rabern — 1/19/99
Date

Approved for the College of Graduate Studies

Bruce R. McLeod, Graduate Dean — Bruce R. McLeod — 1-22-99
Date

STATEMENT OF PERMISSION TO USE

In presenting this thesis in partial fulfillment of the requirements for a doctoral degree at Montana State University-Bozeman, I agree that the Library shall make it available to borrowers under rules of the Library. I further agree that copying of this thesis is allowable only for scholarly purposes, consistent with 'fair use" as prescribed in the U.S. Copyright Law. Requests for extensive copying or reproduction of this thesis should be referred to University Microfilms International, 300 North Zeeb Road, Ann Arbor, Michigan 48106, to whom I have granted "the exclusive right to reproduce and distribute my dissertation in and from microform along with the non-exclusive right to reproduce and distribute my abstract in any format in whole or in part."

Signature 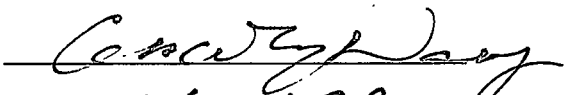

Date 4/15/99

ACKNOWLEDGEMENTS

I would like to express my appreciation to Dr. James D. Bryers for serving as my advisor. His invaluable guidelines, suggestions, and knowledge as well as all the efforts for the arrangements of experiments outside of Montana State University make this dissertation possible. Moreover, his sincere friendship is also greatly appreciated. It is an unique pleasant experience to work for him. Thanks to Drs. Anne Camper, Al Cunningham, Warren Jones, Gordon McFeters, and Bonnie Tyler for serving on my committee. Among these, special thanks go to Dr. Anne Camper, who served as my co-PI in the past a couple of years.

I also appreciate Center for Biofilm Engineering to allow me the opportunity to work with many graduate students from all different fields to explore their knowledge as well as interesting personalities. I am especially indebted to Sara Hendricks and Karen Xu for the precious friendship and all the sharing. Thanks to Larry Gardner to be my "lab partner" for those late nights or all-nighters. And I would like to thank those friends for pulling out my carboys from the autoclave or providing the laughters in my days: Fuhu Xia, Elinor Pulcini, James Odosso, Jordan Peccia, Ace Baty, Calvin Abernathy, *etc.* Although not a Center student any more, Fintan Van Ommen Kloeke should not be forgotten. John Neuman, the "Life Saver" Lab Manager, is especially remembered. With the help from John, my life in the lab became a lot easier.

I would like to thank Dr. Dudley Watkins at University of Connecticut Health Center for his help on the protein iodination.

Dr. Young T. Yeh, my beloved man, is the one who should share most of the credit to push his wife through this Ph.D. degree. I think he should be rewarded a remote-control PWT (Push Wife Through).

I am indebted to my loving parents for their understanding and endless love. Now, it is time to go home. I shall miss the snow in Montana and my beloved Purple G.

TABLE OF CONTENTS

CHAPTER 1 INTRODUCTION 1

1.1 Background 1

1.2 Scope and Objectives 3

CHAPTER 2 LITERATURE REVIEW 5

2.1 Bacterial Specific Adhesion 5

2.2 Fibronectin 8

2.3 Specific Binding between Staphylococci and Fibronectin 12

2.3.1 Microbial FN Receptors 12

2.3.2 Bacterial Binding Domain 14

2.4 Control of Protein Deposition on Substratum 16

2.5 Mathematical Model 17

CHAPTER 3 MATERIALS AND METHODS 20

3.1 Bacterial Strain and Medium 20

3.2 Growth Curve 21

3.3 Flow Cell Reactor and Fluid Dynamics 21

3.4 Proteins 27

3.5 Coupon Preparation and Protein Binding 27

With NH_2 ends tethered on the substratum (COOH-terminal ends exposed) 28

With COOH ends tethered on the substratum (NH_2-terminal ends exposed) 28

3.6 Protein Radiolabeling and Quantitation 29

3.6.1 Bolton-Hunter Reagent 30

3.6.2 NanoOrange™ Protein Assay 31

3.7 Bacterial Adhesion 31

CHAPTER 4 RESULTS 33
4.1 *Staphylococcus epidermidis* Batch Growth Rate Studies 33
4.2 Protein and Peptide Binding Studies 35
4.3 Bacterial Adhesion Studies 38
4.3.1 Control Studies with Clean Glass without Treatment: Experiment Control-I 38
4.3.2 APTES-only coated Control Studies: Experiment Control-II and III 41
Control-II 41
Control-III 45
4.3.3 Adhesion to RGDS-coated Substratum 49
4.3.4 Adhesion to FN-coated Substratum: COOH-End Exposed 57
4.3.5 Adhesion to FN-coated Substratum: NH_2-End Exposed 66

CHAPTER 5 SUMMARY AND DISCUSSION 75
5.1 Protein Immobilization 76
5.2 Protein Quantitation 80
5.3 Specific Adhesion on RGDS-coated Substratum 82
5.4 Specific Adhesion on FN-coated Substratum 83
5.5 Model vs. Experiement 86
5.6 Recommendations for Future Work 94

REFERENCES 95

APPENDICES 105
APPENDIX A Mathematical Model 106
Symbol Nomenclature 111
APPENDIX B NanoOrange™ Protein Assay 113
APPENDIX C Glycerol Assay 117
APPENDIX D Growth Rate Studies 122
APPENDIX E XPS Analysis 126

APPENDIX F Protein Radiolabeling and Quantitation 136

F.1 Coupons Coated with Collected ^{125}I-labelled Protein Solutions 139

F.2 Coupons Coated with Diluted ^{125}I-labelled Protein Solutions 141

F.3 Conversion from Specific Activity into Protein Content 145

FN content determination 145

RGDS content determination 149

APPENDIX G Initial Adhesion Rate Statistics 150

LIST OF FIGURES

Figure 2.1	A scheme representing the receptor:ligand interaction	7
Figure 2.2	Scheme of the structure of a fibronectin dimer	11
Figure 2.3	Pictorial representation of the cell-substratum system	19
Figure 3.1	Flow cell reactor design	22
Figure 3.2	The scheme of laminar flow chamber	23
Figure 3.3	The entire experimental setup	26
Figure 4.1	Growth rate (μ_g) of *S. epidermidis* vs. glycerol concentration	34
Figure 4.2	Linear regression of FN density and FN (^{125}I-FN or unlabeled FN) concentration in solution used for coupon coating	37
Figure 4.3	Bacterial attachment on untreated clean glass coupon over a time period of 3 hours	40
Figure 4.4	Time series of attached cell density on coupons treated with 2% APTES in Control-II	43
Figure 4.5	Time series of attached cell density on coupons treated with 2% APTES in Control-II, plotted the first 10 min of data from Figure 4.2	44
Figure 4.6	Attached cell density on coupons treated with 0.5% and 2% APTES in Control-III	47
Figure 4.7	The plot of the first 10 min of attached cell density on coupons treated with 0.5% and 2% APTES in Control-III	48
Figure 4.8	Attached cell density on coupons coated with RGDS peptide in Experiments R(1) and R(2)	51

Figure 4.9	Attached cell density on coupons coated with RGDS peptide in Experiments R(3) and R(4)	52
Figure 4.10	The plot of the first 10 min of data of attached cell density on coupons coated with RGDS peptide from Figure 4.8	54
Figure 4.11	The plot of the first 10 min of data of attached cell density on coupons coated with RGDS peptide from Figure 4.9	55
Figure 4.12	Attached cell density on coupons coated with FN with COOH-end exposed (FN(1)-(3))	61
Figure 4.13	Attached cell density on coupons coated with FN with COOH-end exposed (FN(3) & (4))	62
Figure 4.14	The plot of the first 10 min of data of attached cell density on coupons coated with FN from Figure 4.12	63
Figure 4.15	The plot of the first 10 min of data of attached cell density on coupons coated with FN from Figure 4.13	64
Figure 4.16	Attached cell density on coupons coated with FN with NH_2-end exposed (FN(5) and (6))	70
Figure 4.17	Attached cell density on coupons coated with FN with NH_2-end exposed (FN(7) and (8))	71
Figure 4.18	The plot of the first 10 min of data of attached cell density on coupons coated with FN from Figure 4.16.	72
Figure 4.19	The plot of the first 10 min of data of attached cell density on coupons coated with FN from Figure 4.17.	73
Figure 5.1	Computer simulation for Experiment FN(8).	88
Figure 5.2	Computer simulation for Experiment FN(7).	89
Figure 5.3	Computer simulation for Experiment FN(6).	90

Figure 5.4	Computer simulation for Experiment FN(5).	91
Figure B.1	Standard protein curve, in terms of fluorescence signal units (fsu) vs. BSA standard concentration	115
Figure B.2	Details of the standard protein curve in Figure B.1 in the range of 10 ng/ml to 1.0 μg/ml.	116
Figure C.1	Glycerol standard curve	120
Figure C.2	Summary of the results of glycerol assay	121
Figure D.1	Growth rate (μ_g) of *S. epidermidis* versus glycerol concentration	124
Figure D.2	The plot of $(1/\mu_g)$ versus (1/[Gly])	125
Figure E.1	High-resolution XPS C1s spectrum of APTES pre-treated glass coupons, with the peak at around 285 eV	128
Figure E.2	High-resolution XPS C1s spectrum of coupons pre-treated with APTES and then submerged in water for 3 hours	129
Figure E.3	High-resolution XPS C1s spectrum of coupons pre-treated with both APTES and glutaraldehyde and then submerged in water for 3 hours	130
Figure E.4	High-resolution XPS N1s spectrum of APTES pre-treated glass coupons	131
Figure E.5	High-resolution XPS N1s spectrum of coupons pre-treated with APTES and then submerged in water for 3 hours	132
Figure E.6	High-resolution XPS N1s spectrum of coupons pre-treated with both APTES and glutaraldehyde and then submerged in water for 3 hours	133
Figure F.1	Gamma readings in cpm on ^{125}I-labeled FN and RGDS.	138

Figure F.2	Calibration curves for Gamma count of ^{125}I-labeled FN and RGDS in PBS	142
Figure F.3	Gamma count from coupons coated with 3 different ^{125}I-FN concentrations	144
Figure F.4	Linear regression of FN density and FN (^{125}I-FN or unlabeled FN) concentration in solution used for coupon coating	148
Figure G.1	Curve fit of Control II-1 data for the initial adhesion rate calculation	152
Figure G.2	Curve fit of Control II-2 data for the initial adhesion rate calculation	153
Figure G.3	Curve fit of Control II-3 data for the initial adhesion rate calculation	154
Figure G.4	Curve fit of Control III-1a data for the initial adhesion rate calculation	155
Figure G.5	Curve fit of Control III-1b data for the initial adhesion rate calculation	156
Figure G.6	Curve fit of Control III-2a data for the initial adhesion rate calculation	157
Figure G.7	Curve fit of Control III-2b data for the initial adhesion rate calculation	158
Figure G.8	Curve fit of R(1)-Control data for the initial adhesion rate calculation	159
Figure G.9	Curve fit of R(1)-100μg data for the initial adhesion rate calculation	160
Figure G.10	Curve fit of R(2)-Control data for the initial adhesion rate calculation	161
Figure G.11	Curve fit of R(2)-100μg data for the initial adhesion rate calculation	162
Figure G.12	Curve fit of R(2)-1mg data for the initial adhesion rate calculation	163

Figure G.13 Curve fit of R(3)-Control data for the initial adhesion rate calculation 164

Figure G.14 Curve fit of R(3)-100μg data for the initial adhesion rate calculation 165

Figure G.15 Curve fit of R(4)-Control data for the initial adhesion rate calculation 166

Figure G.16 Curve fit of R(4)-100μg:1 data for the initial adhesion rate calculation 167

Figure G.17 Curve fit of R(4)-100μg:2 data for the initial adhesion rate calculation 168

Figure G.18 Curve fit of FN(1)-Control data for the initial adhesion rate calculation 169

Figure G.19 Curve fit of FN(1)-high data for the initial adhesion rate calculation 170

Figure G.20 Curve fit of FN(2)-Control data for the initial adhesion rate calculation 171

Figure G.21 Curve fit of FN(2)-high data for the initial adhesion rate calculation 172

Figure G.22 Curve fit of FN(3)-Control data for the initial adhesion rate calculation 173

Figure G.23 Curve fit of FN(3)-med data for the initial adhesion rate calculation 174

Figure G.24 Curve fit of FN(4)-Control data for the initial adhesion rate calculation 175

Figure G.25 Curve fit of FN(4)-low data for the initial adhesion rate calculation 176

Figure G.26 Curve fit of FN(5)-Control data for the initial adhesion rate calculation 177

Figure G.27 Curve fit of FN(5)-med data for the initial adhesion rate calculation 178

Figure G.28 Curve fit of FN(5)-high data for the initial adhesion rate calculation 179

Figure G.29 Curve fit of FN(6)-Control data for the initial adhesion rate calculation 180

Figure G.30 Curve fit of FN(6)-med data for the initial adhesion rate calculation 181

Figure G.31 Curve fit of FN(6)-high data for the initial adhesion rate calculation 182

Figure G.32 Curve fit of FN(7)-Control data for the initial adhesion rate calculation 183

Figure G.33 Curve fit of FN(7)-med data for the initial adhesion rate calculation 184

Figure G.34 Curve fit of FN(7)-high data for the initial adhesion rate calculation 185

Figure G.35 Curve fit of FN(8)-Control data for the initial adhesion rate calculation 186

Figure G.36 Curve fit of FN(8)-med data for the initial adhesion rate calculation 187

Figure G.37 Curve fit of FN(8)-high data for the initial adhesion rate calculation 188

LIST OF TABLES

Table 3.1	Dimensions of the flow chamber	23
Table 3.2	Summary of flow cell operating conditions and hydrodynamic parameters	25
Table 4.1	Coupon pre-treatment information and inlet cell concentration for each run in Control-II Experiments	42
Table 4.2	Increase of attached cell density in percentage at end of 3 hours.	42
Table 4.3	Initial adhesion rates for the first 10 min calculated as the slope from the curves in Figure 4.5	42
Table 4.4	Coupon pre-treatment condition and inlet cell concentration for each run in Control-III Experiments	46
Table 4.5	Decrease of attached cell density in percentage at end of 3 hours for each run in Control-III Experiments when the APTES pre-treatment was decreased from 2% to 0.5%	46
Table 4.6	Initial adhesion rates for the first 10 min calculated as the slope from the curves in Figure 4.7	49
Table 4.7	RGDS coating concentration and inlet cell concentration for each run in RGDS Exp Set	50
Table 4.8	Decrease of attached cell density in percentage from each run in RGDS Exp Set, compared to controls	53
Table 4.9	Initial adhesion rates for the first 10 min calculated as the slope from the curves in Figures 4.10 and 4.11	56
Table 4.10	FN density on 2% APTES pre-treated coupons coated at decreasing FN concentrations, with NH_2 groups tethered on the surfaces	58

Table 4.11	Inlet cell concentration to flow cell in FN Exp with NH_2 groups tethered on the substratum.	58
Table 4.12	Changes in attached cell density, compared to the control coupon in each set, in percentage at the end of 3 hours in FN Exp with NH_2 groups tethered on the substratum	60
Table 4.13	Initial adhesion rates for the first 10 min calculated as the slope from the curves in Figures 4.14 and 4.15	65
Table 4.14	FN density on 2% APTES pre-treated coupons coated with two different FN concentrations, with COOH groups tethered on the surfaces	67
Table 4.15	Inlet cell concentration to flow cell in FN Exp with coupons coated with COOH-groups tethered on the substratum. FN density is also listed	67
Table 4.16	Increase of attached cell density in percentage, compared to the control coupon in each set, at the end of 3 hours in FN Exp with COOH-groups tethered on the substratum	68
Table 4.17	Initial adhesion rates for the first 10 min calculated as the slope from the curves in Figures 4.18 and 4.19.	74
Table 5.1	Comparisons of FN density obtained by passive adsorption found in literature and by immobilization in this dissertation	81
Table 5.2	Ratio of immobilized FN molecules to attached cell number in the experiment of FN(5)-(8), in which NH_2-terminal end of FN was exposed.	85
Table 5.3	Parameter values characterizing the model simulations	87
Table 5.4	Statistical deviations between model prediction and experimental data from FN(5)-(8)	93
Table A.1	Calculated $Root_1$ values for different S_c/R_c.	110

Table E.1	The atomic concentration table of the coupon samples which were pre-treated with APTES only	134
Table E.2	The atomic concentration table of the coupon samples which were pre-treated with APTES only and then submerged in water for 3 hours	134
Table E.3	The atomic concentration table of the coupon samples which were pre-treated with both APTES and glutaraldehyde	135
Table E.4	The atomic concentration table of the coupon samples which were pre-treated with both APTES and glutaraldehyde and then submerged in water for 3 hours	135
Table F.1	Specific activity of ^{125}I-FN coated on coupons pre-treated with 2 different APTES concentrations.	140
Table F.2	Specific activity of ^{125}I-RGDS coated on coupons pre-treated with 2 different APTES concentrations	140
Table F.3	Specific activity of diluted ^{125}I-FN coated on coupons pre-treated with 2 % APTES	143
Table F.4	Conversion of ^{125}I-FN density from the total FN content from Tube no. 10 and the specific activity of ^{125}I-FN coated on coupons pre-treated with 2 % APTES	146
Table F.5	Conversion of FN density from the FN concentrations in solution, labeled and unlabeled, used to coat the coupons pre-treated with 2 % APTES	147

ABSTRACT

Bacterial infection has drawn serious attention in modern medicine, either in respect to biomaterial infection or invasion of tissue surfaces in human bodies. Bacterial adhesion is an essential step in biofilm formation and subsequent infection. Among those factors involved in the complex adhesion process, specific adhesion is a major determinant of cell-cell and cell-substratum adhesions. Currently, the receptor:ligand theory is widely adopted as the governing mechanism of specific cell adhesion.

Staphylococcus epidermidis, a prevailing nosocomial pathogen of biomedical implants and devices, uses the specific adhesion binding with human fibronectin (FN), a glycoprotein found in extracellular matrix and plasma. A FN specific receptor on *S. epidermidis* and the protein FN pair as the receptor:ligand in specific adhesion. This dissertation reports an experimental study of the specific adhesion of *S. epidermidis* cells to fibronectin-coated substrata under uniform shear flow. The effects of ligand density on specific adhesion as well as the binding affinities between bacterial cells and different portions of the ligands were studied. The amount of FN molecule bound on the substratum was verified by radiolabeling. Results revealed that exposed NH_2 functional groups of FN exhibited better binding affinity with *S. epidermidis* cells than to the FN molecule with -COOH functional groups free. Increases in FN density on the substratum with the NH_2 groups exposed to bacterial cells led to increased rates and extent of bacterial adhesion.

A dynamic model, proposed in a previous work, was used to describe bacterial cell adhesion that is mediated by specific receptor:ligand binding. Computer simulations of specific adhesion were carried out by introducing the actual laboratory conditions and experimental parameters into the model to interpret the results. The computer simulations agreed well with the experiments with lower inlet cell concentration, while larger deviations existed in the range of higher inlet cell concentration.

CHAPTER 1

INTRODUCTION

1.1 Background

Bacterial infection has drawn serious attention in modern medicine, either in respect to biomaterial infection or invasion of tissue surfaces in human bodies. All these biomaterial/tissue surfaces are susceptible to bacterial colonization which oftentimes results in invasive bacterial infections. Bacterial adhesion is an essential step in biofilm formation and subsequent infection. Once a biofilm infection has established, it can be extremely difficult to eliminate.

Cells, bacterial and mammalian, adhere with high specificity in many situations. Sufficient evidence suggests that cells possess specific molecules on their surfaces which are able to bind with complementary molecules on a target surface, other cells or tissue surfaces, in a highly selective manner (Jones, 1977; Ofek *et al.*, 1978). Presence of specific molecules on the bacterial cells, called *receptors*, such as cell adhesion molecules (CAMs), lectins, antibodies, and fimbriae are required for this specific cell-cell or cell-surface adhesion (Frazier *et al.*, 1982; Edelman, 1983; Springer and Barondes, 1982; Jann and Jann, 1990). Complementary molecules on the tissue surface are called *ligands*. Specificity of the interaction is a result of specific *receptor:ligand* binding.

Specific adhesion of bacteria has been observed in the intestine of a pig and the human tooth or lung (Costerton *et al.*, 1978). First demonstrated in *Escherichia coli* strains which caused infections of the intestine of newborn pigs, specific adhesion was characterized by the production of an antigen designated K88 (Jones and Rutter, 1972).

Gibbons and van Houte (Gibbons and van Houte, 1971, 1975a, 1975b) observed the selective nature of bacterial adhesion of various oral bacterial species to human and animal epithelial cells *in vitro* and *in vivo*. They concluded *Streptococcus sanguis* and *S. mutans* mostly adhered to the teeth and induced dental caries, while *S. salivarius* colonized the dorsal surface of the tongue. *Pseudomonas aeruginosa* causes lung infection in the disease cystic fibrosis (Lam *et al.*, 1980), and in the bacterial-derived keratitis associated with extended-wear contact lenses (Slusher *et al.*, 1987). Selectivity was also observed in the case of Staphylococci-associated infection. Both being the major elements of the normal skin microflora (Kloos and Musselwhite, 1975), *Staphylococcus aureus* is the most common pathogen in osteomyelitis, whereas *Staphylococcus epidermidis* infects vascular prostheses, total artificial heart, total joints, and orthopedic implants (Masur and Johnson, 1980; Sugarman and Young, 1984; Gristina *et al.*, 1987).

In particular, staphylococcal adhesion to implanted biomaterials represents a major cause of implant failure. Numerous studies have provided much knowledge and understanding of specific adhesion of *S. aureus* (Kuusela, 1978; Doran and Raynor, 1981; Proctor *et al.*, 1982; Rydén *et al.*, 1983; Vann *et al.*, 1984; Proctor 1987; Raja *et al.*, 1990), a coagulase-positive species. Various studies have documented the capacity of coagulase-negative staphylococci (CN-Staph) to adhere to either uncoated or protein-coated biomaterials (Fleer *et al.*, 1990). CN-Staph, especially *S. epidermidis*, is associated with human disease. In many cases, serum protein fibronectin significantly enhances the CN-Staph adhesion which is mediated by specific *receptor:ligand* binding. Compared to the intense research of coagulase-positive *S. aureus*, however, less is known about the specific adhesion mechanism used by *S. epidermidis*.

1.2 Scope and Objectives

This research focused on the specific adhesion of *S. epidermidis* cells onto human fibronectin as a result of specific binding under uniform shear flow. The flow was controlled to study bacterial adhesion as mediated by specific receptor:ligand binding under conditions simulating those in the human vessel. The temperature of experiment was kept at normal human body temperature (37°C). The goal of this study is to understand the mechanism of bacterial specific adhesion by investigating the effects of various ligand densities on specific adhesion as well as the affinities of the binding between bacterial cells and different portions of the ligands. A model developed earlier (Wang, 1993; Wang and Bryers, 1997) to simulate the adhesion experiment was used to interpret results from the experimental work.

The objectives of this work were as follows:

Objective 1:

To establish engineered substratum surfaces with uniform ligand coating in specific ligand orientations.

Objective 2:

To study the effects of various ligand densities on specific adhesion.

Objective 3:

To ascertain the effects of receptor:ligand binding affinities on specific adhesion.

Objective 4:

To compare the experimental results with the predictions achieved from a previous dynamic model.

The following tasks were required to achieve the objectives:

Task 1:

Construct substratum surfaces with various ligand densities as well as different molecular orientations of ligand by manipulating binding of the molecule to the surface.

Task 2:

Carry out bacterial specific adhesion experiments to determine the effects of specific binding with various ligand densities.

Task 3:

Carry out bacterial specific adhesion experiments to certify the effects of different binding affinities.

CHAPTER 2

LITERATURE REVIEW

2.1 Bacterial Specific Adhesion

The ability to attach to surfaces is a property common to almost all bacteria. Pathogenic bacteria may also adhere to and colonize normally sterile surfaces such as the mucosa of the genito-urinary tract and the lower respiratory tract, and endothelial surfaces of the cardiovascular system (Beachey, 1980). Adhesion processes involve complex interactions between bacteria, properties of substratum surface to be colonized, adsorbed substances on the substratum, and the ambient fluid environment (Gristina, 1987). In addition to those factors, receptor:ligand binding, which leads to specific adhesion, is a major determinant of cell-cell and cell-substratum adhesions. Bacteria adhesion to host tissues and biomedical implants is the first step in the process of many bacterial infections and inflammations. In most cases, *receptors, i.e.,* proteins present at the cell surface of bacteria recognize and bind to specific ligands in the host tissue. Currently, the receptor:ligand theory is widely adapted by many researchers as the governing mechanism of specific cell adhesion.

Specific adhesion depends primarily upon the union of the *receptors* with the complementary surface *ligands* (Christensen *et al.*, 1985). Subsequent to or concomitant with initial attachment, cell receptors and surface ligands may interact if they are present within a specific proximity. This idea represents an extension of the "schloss and schlussel" (lock-and-key) hypothesis, which was formulated by Emil Fischer (1894). He used the concept to explain the specificity of interactions between enzymes and their substrates. Paul Ehrlich (1900)

extended this concept to explain the highly specific reactions of the immune system. **Figure 2.1** presents a schematic picture for the receptor:ligand mechanism of bacteria.

The interaction between receptors and ligands must be specific and result in selective adhesion of the bacteria to a surface or to other cells. The first evidence of specific adhesion was from a series of studies by Duguid in the 1950s. He demonstrated that many strains of *Escherichia coli* and related bacteria attached to cells from the epithelial lining of tissues and to erythrocytes, or red blood cells (Duguid *et al.*, 1955; Duguid and Gillies, 1957; Duguid, 1959). Direct evidence for the existence of specific receptors was derived from studies on the pathogenesis of K88-positive ETEC (Enterotoxigenic *E. coli*). ETEC is a major cause of diarrhea in humans and neonatal animals. These strains of *E. coli* extensively colonize the small intestines of neonatal pigs by adhesion and also adhere *in vitro* to purified brush borders prepared from porcine enterocytes. K88-positive ETEC do not colonize the small intestines or adhere to brush borders from resistant pigs (Jones and Rutter, 1972; Sellwood, 1980). The results were explained by the presence of K88 antigens which are the specific ligands.

Today, it is clear that the specificity of bacterial adhesion is a common phenomenon. For instance, group A *Streptococci* adhere only to the upper respiratory tract and skin, and seldom cause urinary tract infections. In contrast, *E. coli* is the most common agent of urinary tract infections, but is rarely found in the upper respiratory tract (Sharon and Lis, 1993).

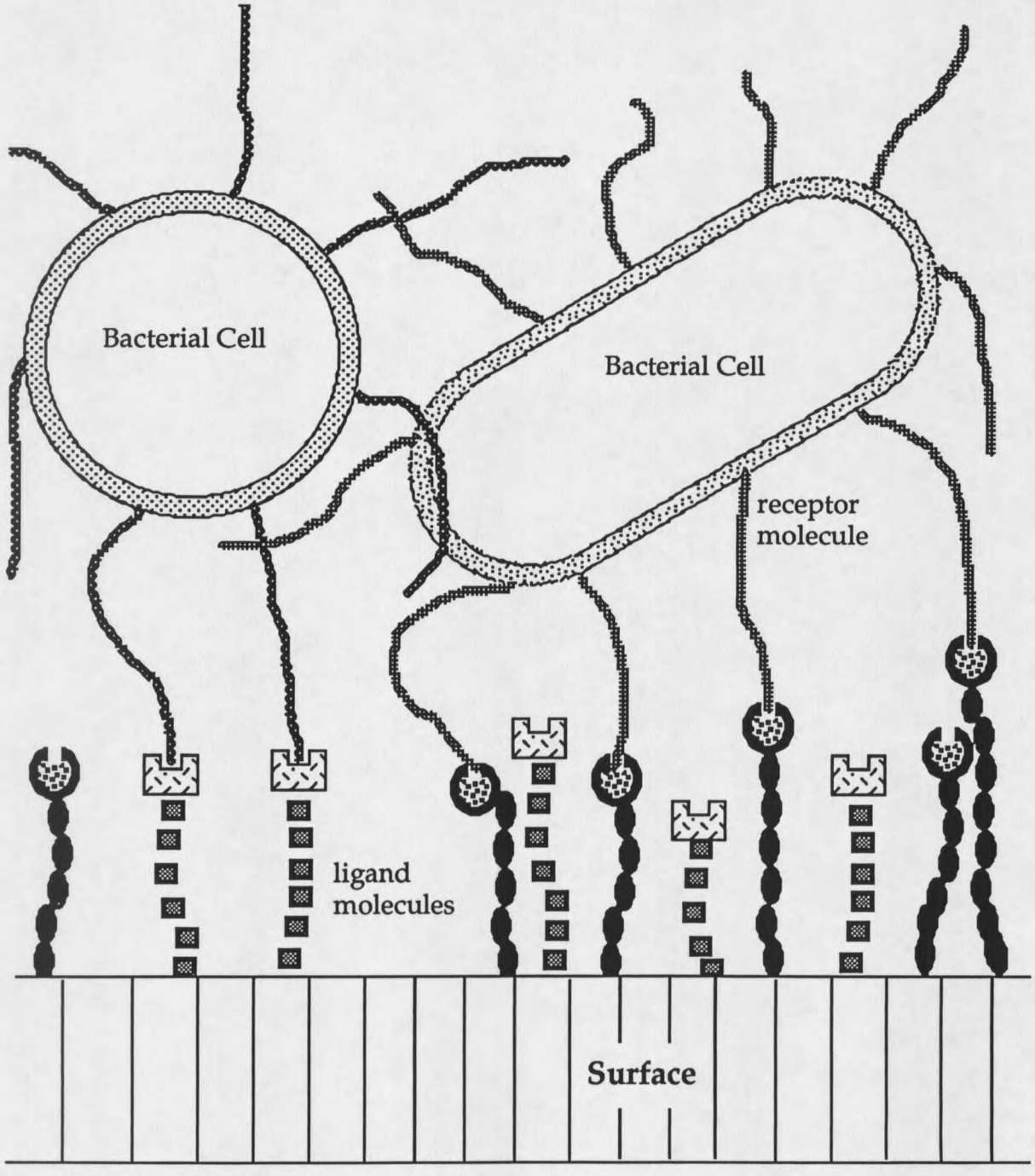

Figure 2.1 A scheme representing the receptor:ligand interaction

In order to cause disease, bacteria must be capable of sticking to the tissue surface in a susceptible host. Those infectious strains lacking the ability to adhere will be swept away from tissues by the host's normal cleansing mechanisms. For example, bacteria in the urinary tract may be flushed out in the urine, and those in the upper respiratory tract might be swallowed and destroyed by stomach acid (Sharon and Lis, 1993). Thus, for bacteria, specific adhesion provides the advantage of firm attachment to tissue surfaces allowing the bacteria to withstand the cleansing action of the host, *e.g.*, mucous flow, ciliary movement, sneezing, cough, urination, peristalsis, swallowing, *etc* (Christensen *et al.*, 1985).

Receptors may interact with a broad variety of ligands or may only bind to very specific ligands (Christensen *et al.*, 1985). Therefore, the "fit" of the receptor:ligand interaction directly determines the range of suitable substrata for bacteria to attach. In some systems, bacteria employ more than one type of receptor to bind with tissues. Multiple adhesive systems require the targeted surfaces to display more than one kind of ligand before optimal adhesion takes place. This rigid criterion restricts the chances of coincidental adhesion to non-targeted tissues and enable bacteria to adhere to a range of host species and tissues (Isaacson, 1985).

2.2 Fibronectin

Fibronectin (FN), a prototype cell adhesion protein, is a multifunctional extracellular matrix and plasma protein that plays a central role in both mammalian and bacterial cell adhesion. Fibronectin is a glycoprotein with a molecular weight of about 440 kilodaltons (kD) that supports cell migration during a variety of biologically important processes, such as hemostasis, wound healing, embryonic development, and tumor cell invasion (Humphries *et al.*, 1991). The plasma fibronectin molecule is a dimer which consists of two similar polypeptides bridged together through two disulfide bonds near the COOH-terminal ends. The dimer structure of fibronectin is shown schematically in **Figure 2.2** (Alberts *et al.*, 1989). Various domains of FN play different roles in

binding with various molecules, *e.g.*, collagen (Furie and Rifkin, 1980), heparin (Yamada *et al.*, 1980), and eukaryotic cells (Ruoslahti and Hayman, 1979), as shown in Figure 2.2.

FN from different sources exhibits slight differences in the molecular weights of the polypeptides. FN isolated from plasma consists of polypeptides that differ from one another in molecular weight and that are distinctly smaller than those produced by most types of cultured cells, *i.e.*, "cellular" FN (Yamada and Kennedy, 1979). Unlike other types of culture cells, early cultures of hepatocytes synthesize FN that has the same polypeptide composition as plasma FN. This indicates that the liver is the source of plasma FN (Tamkun *et al.*, 1984).

The amount of carbohydrate of FN also differs, depending on the source of the protein. In general, FN contains 4-10 % carbohydrate (Ruoslahti, 1988). FN from embryonal sources and tumor cells contain more sugar, while FN from adult plasma and from cultured normal adult skin fibroblasts has a relatively low carbohydrate content (Fukuda and Hakomori, 1979).

Early studies identified a large protease fragment from the center of the FN molecule that retained eukaryotic cell binding activity. The eukaryotic cell binding domain primarily involves a specific tetrapeptide sequence, Argenine-Glycine-Aspartic-Serine (Arg-Gly-Asp-Ser: RGDS), which subsequently was found in cell binding sites of several other adhesive matrix glycoproteins (Pierschbacher and Ruoslahti, 1984; Ruoslahti and Pierschbacher, 1986). Peptides containing this sequence promote cell adhesion directly and inhibit cell adhesion to FN, while analogs containing conservative changes such as Arg to Lys (Lysine) or Asp to Glu (Glutamic acid) are inactive. When these peptides are coupled to a solid surface, they promote the adherance of eukaryotic cells to that surface. Synthetic peptides containing the RGD sequence compete with FN and block the adhesion of eukaryotic cells to a substratum coated with FN or the peptides themselves (Pierschbacher and Ruoslahti,

1984; Yamada and Kennedy, 1984). The RGDS sequence is characterized as the binding site for eukaryotic cells and a family of eukaryotic receptors recognizing RGDS sequence in matrix protein has been identified (Hynes, 1987). This receptor family is named "integrins". The members of the intergrin superfamily are typically heterodimers of two subunits α and β (Ruoslahti and Pierschbacher, 1987). The α subunit consists of two polypeptides disulfide-linked to one another. The β subunit is a single polypeptide with a molecular weight of about 140,000.

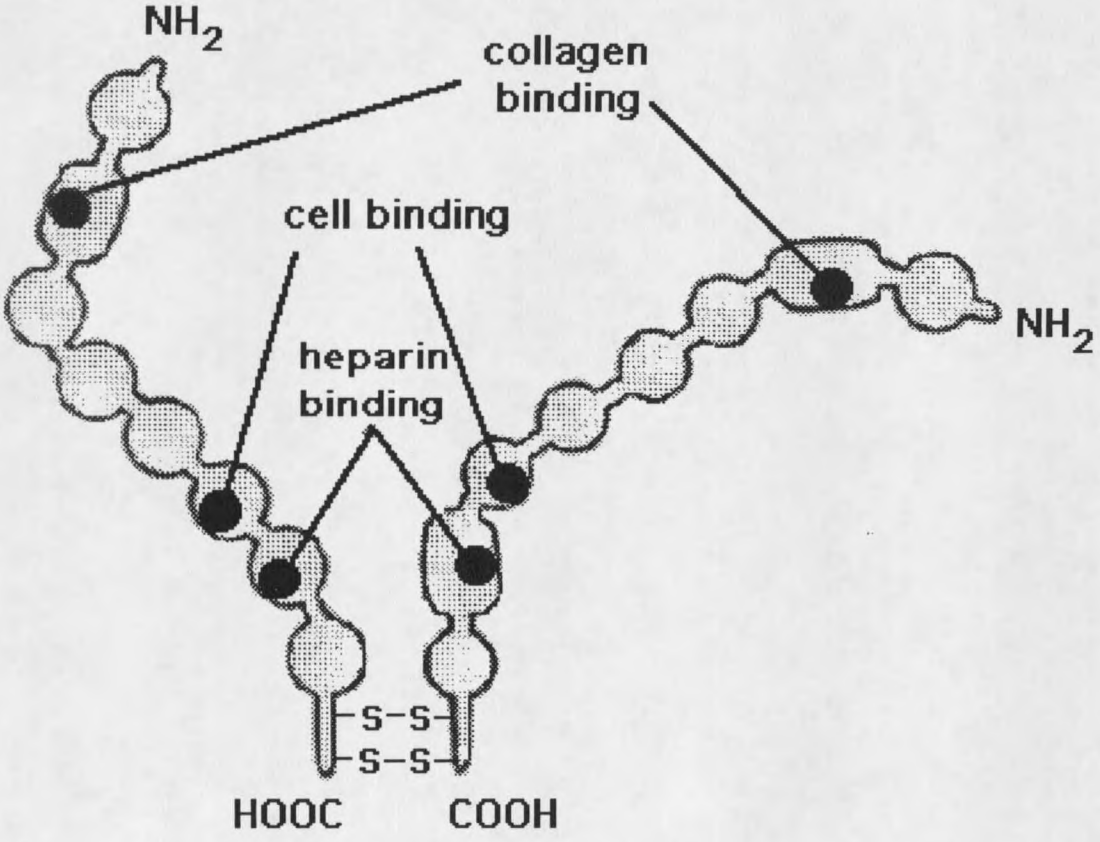

Figiure 2.2 Scheme of the structure of a fibronectin dimer.

2.3 Specific Binding between Staphylococci and Fibronectin

Fibronectin, which comprises approximately 0.5% of the protein in plasma (Yamada and Olden, 1978), interacts with several kinds of macromolecules, cells, and bacteria, which include various strains of staphylococci, and several species of streptococci. *In vitro* studies have shown that staphylococci can bind intact fibronectin molecules or adhere to fibronectin adsorbed on glass or plastic (Kuusela, 1978; Verbrugh *et al.*, 1981; Kuusela, *et al.*, 1984; 1985; Maxe *et al.*, 1986; Russell *et al.*, 1987). Preincubation of bacteria with fibronectin fragments containing the staphylococcal binding site reduced the number of bacterial cells attaching to the fibronectin-absorbed substrata (Kuusela, *et al.*, 1985; Maxe *et al.*, 1986). Russell *et al.*(1987) reported preincubation of PVC catheter segments in fibronectin significantly increased the binding of *S. aureus* and *S. epidermidis*.

2.3.1 Microbial FN Receptors

Studies on microbial FN receptors mostly focused on *S. aureus* receptors. *S. aureus* is the preeminent pathogen for metallic biomaterial and compromised tissues associated with surgical wounds, trauma and osteomyelitis. Digestion of bacteria with trypsin results in loss of fibronectin binding activity. This indicates the bacterial FN binding component is located on the cell surface and is of protein in nature (Ryden *et al.*, 1983). Espersen and Clemmenen (1982) and Fröman *et al.* (1987) isolated a protein from the *S. aureus* Newman strain and identified this cell wall-associated protein as an FN receptor, with a molecular mass of 210 kD. Further, two distinct but related genes encoding the FN-binding proteins (FNbps) from *S. aureus* strain 8325-4 were cloned from a gene bank in vector pBR322 (Flock *et al.*, 1987; Signäs *et al.*, 1989). These two tandem genes, *fnbA* and *fnbB*, corresponding to the proteins FNbpA and FNbpB, are separated by 682bp. The ability of FNbp to bind FN was localized to a 37 or 38 amino acid motif, named the D-motif, which is repeated three times (coded as D1, D2, and D3) and

partially a fourth time (Signäs *et al.*, 1989; McGavin, *et al.*, 1991). Synthetic peptides mimicking each of the three D-motifs, D1, D2, and D3, or their recombinant have been employed in research as receptor analogs to study their FN-binding activities (Signäs *et al.*, 1989; Raja *et al.*,1990; McGavin and Höök, 1995; Huff *et al.*, 1994; Sun *et al.*, 1997). Results showed the synthetic peptides D1, D2, and D3, were able to inhibit FN binding to staphylococcal cells, and peptide D3 showed activity which was 10-fold greater than either D1 or D2 (Signäs *et al.*, 1989). A mixture of D1, D2, and D3 at equimolar ratio was not more active than the individual peptides at similar concentrations (Höök *et al.*, 1988). A genetically constructed chimeric protein, ZZ-FR (molecular mass: 63 kD), containing two immunoglobulin G (IgG)-binding domains of staphylococcal protein A and FN-binding repeats with D1, D2, and D3 sequences per molecule, was found to have a much higher affinity for FN than the individual peptide did (Signäs *et al.*, 1989). ZZ-FR inhibited the attachment of staphylococcal cells to microtiter wells coated with intact FN or with the 29-kD amino-terminal fragment of FN. The recombinant fusion protein ZZ-FR also partially inhibited the adherence of staphylococci to human plasma clots formed *in vitro* but had no effect on bacterial adhesion to clots formed from FN-depleted plasma (Höök *et al.*, 1988; Raja *et al.*, 1990).

Specificity of D3 binding with the 29 kD N-terminal fragment with high affinity was further illustrated in the work of Huff (Huff *et al.*, 1994). It was reported the C-terminal half of D3, when immobilized, selectively adsorbed the 29 kD fragment from a thermolysin digest of FN.

Insertion mutations were isolated in both *fnbA* and *fnbB* genes to study the expression of *fnb* genes in *S. aureus* and to test if both FNbpA and FNbpB proteins are required to promote bacterial adhesion to FN-coated surfaces (Greene *et al.*, 1995). Meanwhile, a double *fnbAfnbB* mutant was also constructed and the influence of this double mutant on bacterial adhesion from was examined. Results revealed the *fnbA* and *fnbB* single mutants showed no significant reduction in their adhesion

to polymethylmethacrylate (PMMA) coverslips coated *in vitro* with FN. However, the double mutant was completely defective in adhesion. Monospecific antibodies directed against the non-conserved amino-terminal regions of both proteins confirmed the lack of expression of FNbps in the mutant strains. Wild-type *fnbA* and *fnbB* genes were able to fully restore the adhesion-defective phenotype of the *fnbAfnbB* mutant. This demonstrated that both genes are expressed in *S. aureus* and both contribute to the ability of *S. aureus* strain 8325-4 to adhere to FN-coated surfaces.

The regulation of FN receptor expression is complicated. The number of FN receptors expressed on bacterial cells is dependent on the phase of growth, the pH of the growth medium, and the types of media. For some bacterial species, prolonged cultivation in the laboratory may result in loss of FN receptor expression (Höök *et al.*, 1989). The composition of the media used to grow bacteria may also extensively affect the FN-binding capicity of the bacteria. Research has shown that *S. aureus* harvested in the logarithmic phase of growth express more FN receptors than do those harvested in stationary phase (Proctor *et al.*, 1982). Based on this, the bacterial cells used in this study were always harvested in logarithmic growth phase.

The number of FN-binding receptor sites per staphylococcal cell has been estimated to range from as few as 5 to more than 20,000 (Proctor *et al.*, 1982; Ryden *et al.*, 1983; Höök et *al.*, 1988).

2.3.2 Bacterial Binding Domain

Earlier work (Mosher and Proctor, 1980) has shown that the primary binding site on FN for staphylococcal cells is located in the N-terminal region which consists of five "fingers" structures (because of the resemblance of fingers on a hand in current schematic representation) of Type I homology repeats (Petersen *et al.*, 1983).

However, a second domain containing three Type I units in the COOH-terminal region has also been proposed (Hayashi and Yamada, 1981) and reported to bind to staphylococcal cells (Kuusela, *et al.*, 1984). The multiple finger domains are crucial in the FN:*S. aureus* binding. Sottile *et al.* (1991) demonstrated that mutation or deletion of any of the first five domains in a recombinant 70 kD N-terminal fragment of FN would strongly reduce or destroy its ability to bind *S. aureus*.

It was suggested (McGavin and Höök, 1995) that FN binding proteins from different genera of Gram-positive bacteria have a common mechanism of ligand binding, most probably associated with recognition of a conserved structural feature within the 29 kD N-terminal domain of FN. It is likely that the binding domain on FN for *S. epidermidis*, a Gram-positive strain, is located within the same region (Höök, personal discussion).

Formerly considered a harmless organism, *S. epidermidis* has been recognized as a significant nosocomial pathogen associated with implants, particularly prosthetic cardiac valves, cardiac pacemakers, intravascular catheters, total artificial hearts, total joints, and orthopedic implants (Wilson *et al.*, 1973; Masur and Johnson, 1980; Wilson *et al.*, 1982; Sugarman and Young, 1984; Linares *et al.*, 1985; Gristina *et al.*, 1987). In patients with prosthetic cardiac valves, the rate of infection is about 1-4%. In those with vascular grafts, the rate is up to 6% (Schoen, 1989). One study reported that FN does not bind to the clinical isolate of *S. epidermidis* (Doran and Raynor, 1981), while another study concluded that a clinical isolate of *S. epidermidis* binds to the COOH region of FN (Holmes *et al.*, 1997). Until now, the binding domain of *S. epidermidis* on fibronectin remains controversial and is not yet determined. The work presented in this dissertation investigated the binding affinities of *S. epidermidis* cells with NH_2 and COOH regions of FN in order to understand the mechanism of the attachment of *S. epidermidis* cells to immobilized FN. The approach of this work is to control the orientations of ligand molecules on the substrata to verify the binding

affinities of those two regions with *S. epidermidis* cells, *e.g.*, to tether the intact FN molecules on the testing coupons in a way that either NH_2 or COOH regions will be available to the bacterial cells in a flowing system.

2.4 Control of Protein Deposition on Substratum

Substratum chemistry affects the attachment of bacteria to solid surfaces. Surface chemistry becomes more influential if protein adsorption takes place. Adsorption of proteins occurs almost instantaneously when a solid surface comes into contact with a protein solution (Wahlgren and Arnebrant, 1991). The protein film formed on the surface may then act as a substratum for subsequent bacterial adhesion. The manner in which the protein molecules adsorb on the substratum has a substantial impact on bacterial attachment. Biological activity of proteins on the surface will depend on whether specific active peptide sequences in specific proteins are accessible to the cells. A well-defined surface with a functional protein layer of specific peptide sequences, rather than random protein adsorption, is essential to study protein:bacteria binding.

The self-assembled monolayer (SAM) technique is one of the technologies used to make nanofabricated engineered surfaces. SAMs with different exposed functional groups which will bind to specific domains of proteins can be produced. Subsequently, a uniform layer of oriented protein will be established. The components that typically make up a self-assembled film are: a substratum (most often smooth on the nanometer scale), an anchor group that interacts with the substratum, and a structure that will assemble (*e.g.*, alkanethiol or alkanesilane), and a head group pointing away from the substratum and providing specificity (Ratner, 1993). The advantages of SAMs are their molecular perfection, resistance to contamination, ease of preparation, and flexibility in permitting a wide range of structures that demonstrate specific interactions.

Wiencek and Fletcher (1995) studied the bacterial adhesion to SAMs built from alkanethiols to produce a range of substrata with two different exposed functional groups--methyl and hydroxyl groups--and also a series of mixtures of these two. These SAMs exhibited various substratum compositions and wettabilities, ranging from hydrophilic, hydroxyl-terminated monolayers to a hydrophobic, methyl-terminated monolayer. They reported the greatest numbers of attached bacterial cells on hydrophobic surfaces and the percentage of cells desorbed between measurements decreased with increasing substratum hydrophobicity.

Glasses and oxidized polymers can be treated with bifunctional silanating reagents to generate surfaces containing alkyl halides, epoxides, thiols, amines or carboxylic acids (Massia and Hubbell, 1991; Pope *et al.*, 1993; Bhatia *et al.*, 1989; Ferguson *et al.*, 1993; Drumheller and Hubbell, 1995). In this dissertation, the alkanesilane approach was adopted.

2.5 Mathematical Model

Previous work (Wang, 1993; Wang and Bryers, 1997) proposed a mathematical model simulating the time course of bacterial adhesion governed by the specific adhesion mechanism. **Figure 2.3** presents an illustration of the cell-substratum system in this model. This model took account of the processes of attachment, detachment, and growth of attached bacteria, as well as the shear force which results in the rotational and translational motions of the bacterial cells in flow. The bacterial cell is modeled as a sphere of radius R_C which is covered evenly with R_T number of receptors on the cell surface. The ligand density on the deposition surface is N_l. Upon close approach to the surface, a contact area for binding is formed on the bacterial cell. The contact area is assumed to be a disk of radius a and is assumed to remain constant as 10% of the cell radius R_C throughout the adhesion period. Details of the model are provided in **Appendix A**.

First-order kinetics were used to express the adhesion rate, detachment rate, and growth rate on the substratum in this model. A relatively short time span for bacterial attachment experiments was deliberately chosen to focus on the study in early stage of attachment only. Thus, growth of any attached cells on the substratum did not dominate net cell accumulation. The experimental data were compared with the predicted results from the model simulations, by adopting real parameters from the laboratory work.